STEM CELLS AND DEVELOPMENT
Volume 22, Number 23, 2013

DOI: 10.1089/scd.2013.0108

N-Glycosylation Profile of Undifferentiated and Adipogenically Differentiated Human Bone Marrow Mesenchymal Stem Cells: Towards a Next Generation of Stem Cell Markers

Houda Hamouda,[1,2,*] Mujib Ullah,[3,*] Markus Berger,[1] Michael Sittinger,[3] Rudolf Tauber,[1] Jochen Ringe,[3] and Véronique Blanchard[1]

Mesenchymal stem cells (MSCs) are multipotent cells that are easy to isolate and expand, develop into several tissues, including fat, migrate to diseased organs, have immunosuppressive properties and secrete regenerative factors. This makes MSCs ideal for regenerative medicine. For application and regulatory purposes, knowledge of (bio)markers characterizing MSCs and their development stages is of paramount importance. The cell surface is coated with glycans that possess lineage-specific nature, which makes glycans to be promising candidate markers. In the context of soft tissue generation, we aimed to identify glycans that could be markers for MSCs and their adipogenically differentiated progeny. MSCs were isolated from human bone marrow, adipogenically stimulated for 15 days and adipogenesis was verified by staining the lipid droplets and quantitative real time polymerase chain reaction of the marker genes peroxisome proliferator-activated receptor gamma (*PPARG*) and fatty acid binding protein-4 (*FABP4*). Using matrix-assisted laser desorption-ionization-time of flight mass spectrometry combined with exoglycosidase digestions, we report for the first time the N-glycome of MSCs during adipogenic differentiation. We were able to detect more than 100 different N-glycans, including high-mannose, hybrid, and complex N-glycans, as well as poly-*N*-acetyllactosamine chains. Adipogenesis was accompanied by an increased amount of biantennary fucosylated structures, decreased amount of fucosylated, afucosylated tri- and tetraantennary structures and increased sialylation. N-glycans H6N5F1 and H7N6F1 were significantly overexpressed in undifferentiated MSCs while H3N4F1 and H5N4F3 were upregulated in adipogenically differentiated MSCs. These glycan structures are promising candidate markers to detect and distinguish MSCs and their adipogenic progeny.

Introduction

Due to their restoration ability, stem and progenitor cells offer a promising cell source for the application in regenerative medicine, whereupon the main goal is to establish methods for the regenerative treatment of diseased or damaged tissues and organs [1]. However, application of pluripotent cells, such as embryonic stem cells or induced pluripotent progenitor cells faces complex difficulties like the formation of teratoma. Multipotent stem and progenitor cells are therefore, a remarkable alternative to fulfill the therapeutic expectations [2].

Bone marrow mesenchymal stem cells (MSCs), presently also referred to as mesenchymal stromal cells, are non-hematopoietic adult multipotent cells. They are easy to isolate and expand and develop into a variety of tissues, including fat, bone, and cartilage [3]. These cells also migrate to diseased organs [4,5], have strong immunosuppressive properties and secrete regenerative factors [6]. Therefore, MSCs are promising for application in cell-based therapy. In first clinical approaches they are administered to patients with hematological pathologies, cardiovascular diseases, osteogenesis imperfecta, musculoskeletal disorders, lung diseases and diabetes [7]. Moreover, MSCs and their adipogenically differentiated progeny also play a role in the regenerative treatment of burn and tumor patients and in cosmetic surgery [8]. The primary source of MSCs is bone marrow, but adipose tissue, synovium, periosteum, amniotic

[1]Institute of Laboratory Medicine, Clinical Chemistry and Pathobiochemistry, Charité-Universitätsmedizin Berlin, Berlin, Germany.
[2]Department of Biology, Chemistry and Pharmacy, Freie Universität Berlin, Berlin, Germany.
[3]Tissue Engineering Laboratory and Berlin-Brandenburg Center for Regenerative Therapies, Department of Rheumatology and Clinical Immunology, Charité-Universitätsmedizin Berlin, Berlin, Germany.
*These two authors contributed equally to this work.

fluid, placenta, and umbilical cord blood also contain MSCs and can therefore, be used as alternative cell sources [9].

For practical reasons, such as to verify homogeneous MSC cultures or to monitor the quality and progress of MSC differentiation during repair tissue formation, and to fulfill regulatory issues like therapy approval, knowledge of biomarkers describing MSCs, and their development stages is of utmost importance. However, all known MSC markers, among them the most prominent ones like the cell surface proteins CD73 (5′-nucleotidase), CD90 (thy-1), CD105 (endoglin), CD166 (alcam) [3] and Stro-1 [10] are not specific. For instance, MSCs are usually identified as colony-forming unit-fibroblasts and Stro-1 negative cells are not capable of forming colonies [11]. In contrast, Stro-1 positive cells are capable to become hematopoietic stem cell-supporting fibroblasts, smooth muscle cells, adipocytes, osteoblasts, and chondrocytes, which support the functional role of MSCs. In addition, Stro-1 is not only expressed from MSCs and its expression is gradually lost during culture. Several other useful but unspecific markers for MSCs and their differentiated progeny have been identified in molecular profiling approaches for example focusing on the adipogenic lineage [12]. Knowledge of markers for precise labeling and tracking of those cells would therefore, strongly enhances their importance in regenerative medicine.

Most of the known molecular markers of cells are cell surface proteins or lipids. In addition to proteins and lipids, carbohydrates are the next major class of cellular macromolecules and are at the same time abundant components of the cell surface. Indeed, many stem cell markers possess a crucial carbohydrate epitope, which is involved in many aspects of stem cell biology, such as proliferation and differentiation [13]. Moreover, their cell surface position and lineage-specific nature makes them ideal to identify and isolate specific cell types [13].

Carbohydrates are referred to as glycans that are covalently linked to membrane proteins or lipids and form a dense glycocalyx on the extracellular side of the surface of all cells found in multicellular animals, including stem cells. Cell surface glycans are optimally positioned to help the cell to communicate with its extracellular environment and are the main components of the glycocalyx [14,15]. Since they form the outermost layer of the cell, cell surface glycans act as recognition elements and binding sites. Thus, they are the first molecules that are encountered by antibodies, hormones, viruses, bacteria, toxins, and other cells. Moreover, cell surface glycans are capable of orienting the binding faces of cells to facilitate cell adhesion and they can prevent nonspecific protein–protein interactions [16,17]. Besides the fact that glycans are involved in the regulation and control of protein folding and trafficking, cell surface glycans play important roles in the interaction of stem cells with their niche and are able to modulate the growth and differentiation of stem cells in vitro [13,18].

Co- and post-translational modification of proteins through glycosylation is an enzymatically driven process which takes place in the endoplasmatic reticulum and in the Golgi apparatus where the extent and type of glycosylation is determined by the cell type, as well as the species. As an example, N-glycosylation is a common protein post-translational modification occurring on asparagine residues of the consensus sequence asparagine-X-serine/threonine, where X may be any amino acid except from proline. Since different cell types express different glycan signatures, glycans are promising targets for the identification of stem cell markers [13,19–21]. They possess a broad structural variation whereby their characteristic molecular structures carry vast amounts of biological information [15]. The specific structures expressed on the cell surface can be indeed helpful in understanding their function and role during differentiation of stem cells.

Several studies revealed stem cell markers mainly for embryonic, hematopoietic and neural stem cells that are identified through their carbohydrate antigens [22–24]. For instance, the glycolipids SSEA-3 and SSEA-4, which are typically used as embryonic stem cell markers, were originally identified through monoclonal antibodies recognizing carbohydrate epitopes that are part of globoseries glycosphingolipids [13,24]. Polysialylated neuronal cell adhesion molecule is considered as a neural cell surface stem cell marker, which is modified with a linear homopolymer consisting of α(2–8)-linked sialic acid molecules and is mainly expressed in the developing nervous system [25,26].

To study adipogenesis [12] in the context of obesity research and soft tissue engineering [8], MSCs are routinely stimulated into the adipogenic lineage. In this view, (bio) markers are important to verify culture homogeneity of MSCs and their adipogenically differentiated progeny, to monitor the progress of MSC development during adipogenesis and to determine the quality (like cell distribution) of the new formed adipose tissue. Thus, in the present study we aimed at investigating development stage-specific glycan markers by comparing the qualitative and quantitative N-glycome of undifferentiated and 5 and 15 days adipogenically differentiated human MSCs. To this end, we first performed standard adipogenic differentiation assays. Then, cell membrane glycoproteins were isolated and N-glycans were released and analyzed by matrix-assisted laser desorption-ionization-time of flight mass spectrometry (MALDI-TOF-MS) combined with exoglycosidase digestions. We report over 100 N-glycan structures and that adipogenesis is accompanied by an increased amount of biantennary fucosylated structures, decreased amount of fucosylated, afucosylated tri- and tetraantennary structures, and increased sialylation. N-glycans like H6N5F1 and H7N6F1 were significantly overexpressed in undifferentiated MSCs, whereas H3N4F1 and H5N4F3 were increased in adipogenically differentiated MSCs. This provides the basis for further studies to identify the core peptides of the candidate N-glycans, which would facilitate subsequent antibody production and easy detection of the new glycan-based markers.

Materials and Methods

Isolation and culture expansion of human MSCs

MSCs were isolated from iliac crest bone marrow aspirates of three informed and consenting donors ($n = 3$ males, average age: 59 ± 12.28 years), who were examined to exclude hematopoietic neoplasms. The ethical committee of the Charité-University Medicine Berlin approved the study. Briefly, aspirates were mixed with MSC expansion medium consisting of Dulbecco's Modified Eagle's Medium (DMEM; Biochrom) supplemented with 10% fetal bovine serum (FBS; Thermo Scientific Hyclone), 2 ng/mL basic fibroblast

growth factor (PeproTech), 2 mM L-glutamine, 100 U/mL penicillin and 100 μg/mL streptomycin (all Biochrom), and were seeded at a density of 2×10^5 nucleated cells per cm^2. After 2 days, nonadherent cells were washed out by the first media exchange. During cell expansion up to passage 3 (P3), culture medium was changed three times per week and upon attaining 90% confluence, cells were detached by the addition of 0.05% trypsin/1 mM ethylenediaminetetraaceticacid (EDTA; both Biochrom) and replated at a density of 5×10^3 cells per cm^2. Cell number was calculated and cell viability was determined based on trypan blue staining of detached cells.

Flow cytometric analysis of human MSCs

P3 cells from all three donors were examined for their MSC cell surface antigen expression pattern. Briefly, for each fluorescence-activated cell sorting (FACS) analysis, 2.5×10^5 cells were washed, centrifuged (5 min at 250 *g*) and resuspended in cold phosphate-buffered saline (PBS)/0.5% bovine serum albumin (BSA; Biochrom). Cells were incubated for 15 min on ice with R-phycoerythrin-labeled mouse anti-human CD14, CD34, CD73, or CD166, or fluorescein isothiocynate labeled mouse anti-human CD44, CD45, CD90, or CD105 antibodies. All antibodies were purchased from BD-Pharmingen with the exception of CD105 antibody, which was purchased from Acris Antibodies. After incubation, cells were centrifuged, washed and re-suspended in PBS/0.5% BSA. Propidium iodide (100 μg/mL; Sigma-Aldrich) staining was applied for the exclusion of dead cells, while unstained cells were used as a negative control. The cells were analyzed with a FACSCalibur flow cytometer (Becton Dickinson) and the results were evaluated using CellQuest software.

Adipogenic differentiation of human MSCs

To determine the N-glycome of adipogenically differentiated MSCs, 1×10^4 P3 MSCs ($n=3$ donors) were seeded per cm^2 and when reaching postconfluence, were incubated for 3 days in adipogenesis induction medium followed by 2 days in adipogenesis maintenance medium in three consecutive cycles. Maintenance medium was composed of DMEM (4.5 g/L glucose) supplemented with 10% FBS, 100 U/mL penicillin, 100 μg/mL streptomycin and 10 μg/mL insulin (Novo Nordisk). Adipogenesis induction medium contained additionally 1 μM dexamethasone, 0.2 mM indomethacin and 0.5 mM 3-isobutyl-1-methylxanthine (all Sigma-Aldrich). Adipogenesis was documented by oil red O staining (Roth) of lipid droplets and by quantitative real time polymerase chain reaction of adipogenic marker genes, fatty acid binding protein-4 (*FABP4*), and peroxisome proliferator-activated receptor gamma (*PPARG*).

Isolation of adipogenically differentiated human MSCs

To study the N-glycosylation profile of adipogenically differentiated MSCs, P3 MSCs ($n=3$ donors) were adipogenically differentiated for up to 15 days. Differentiated vital cells were isolated from their extracellular matrix by incubation with 0.05% trypsin/1 mM EDTA in PBS for 8 min and 37°C. Afterwards, the cells were washed with PBS, and then centrifuged at 300 *g* for 6 min and 37°C. The washing and centrifugation steps were repeated three times. Cell number was calculated and cell viability was determined based on trypan blue staining of detached cells.

Isolation of RNA and qPCR

To isolate total RNA, undifferentiated and adipogenically differentiated MSCs were homogenized with TriReagent [27]. Then, 1-bromo-3-chloro-propane (Sigma-Aldrich) was added followed by centrifugation (45 min, 13,000 *g*). The aqueous phase was collected and mixed with ethanol. Further steps were performed using the RNeasy Mini Kit (Qiagen).

Afterwards, 2.5 μg of total RNA was reverse transcribed using the iScript cDNA synthesis kit (BioRad). TaqMan quantitative real-time polymerase chain reaction was performed in triplicates in 96-well optical plates on a Mastercycler® ep realplex^2 S system (Eppendorf) with gene expression assays for TaqMan probes and primer sets (Applied Biosystems). Quantitative gene expression analysis was performed for the fat marker genes *FABP4* (Hs01086177_m1) and *PPARG* (Hs01115513_m1). Glyceraldehyde-3-phosphate dehydrogenase (*GAPDH*, Hs99999905_m1) was used as housekeeping gene. Expression values were normalized to the endogenous *GAPDH* expression level and calculated with the $2^{-\Delta\Delta Ct}$ formula in percent expression of *GAPDH* [28].

Isolation of membrane glycoproteins by membrane extraction

Approximately $4.3–13.3\times10^6$ cells per cell type were collected for isolation of membrane glycoproteins. The cells were pelleted and frozen in 100 μL PBS at −80°C until analysis. Membrane extraction was performed according to Lieke et al. [29]. Cell pellets were thawed and suspended in 2 mL of homogenization buffer (pH 7.6), consisting of 1 mM $NaHCO_3$ (Merck), 150 mM KCl, 2 mM $CaCl_2$ (both Roth) and protease inhibitors (EDTA-free; Roche Applied Science). Cell lysis was then performed by 30 strokes through a syringe having a narrow needle, and subsequently 20 mL of 1 mM $NaHCO_3$ (pH 7.6) was added. The cell lysate was centrifuged at 1,400 *g* for 30 min at 4°C and the pellet was discarded. The supernatant, which contains cellular membranes, was then collected and centrifuged at 48,000 *g* for 20 min at 4°C. The resulting pellet, which contains glyco- and other membrane proteins, was washed thrice with 300 μL of water (26,000 *g*, 15 min, 4°C). The pellet was redissolved in water, methanol and chloroform (3:8:4) and incubated for 30 min on ice to separate lipids from membrane proteins. Sonication for 10 min and periodic shaking were performed and proteins were finally pelleted by centrifugation at 26,000 *g* for 20 min at 4°C. The supernatant was discarded and proteins were washed twice with 400 μL of ethanol (26,000 *g*, 10 min, 4°C) and subsequently resuspended in 20 mM NaH_2PO_4/Na_2HPO_4 buffer (pH 7.0; Merck), containing 2% sodium dodeyl sulphate (Serva) and 2% NP-40 (Merck). Detergents were removed overnight using Calbiosorb™ adsorbent beads (Merck, Calbiochem) and the supernatant was assayed for protein concentration by the bicinchoninic acid assay (Thermo Scientific) and finally lyophilized.

Enzymatic release and isolation of N-glycans from cell membrane glycoproteins

Membrane proteins, including glycoproteins were dissolved in 300 μL of 20 mM NaH_2PO_4/Na_2HPO_4 buffer (pH 7.0), and 20 μL of 1 μg/μL trypsin (Sigma-Aldrich) was added to the sample and incubated for 6 h at 37°C. Additional 20 μL of fresh trypsin solution were added and further digestion was carried out overnight at 37°C. After trypsin deactivation (99°C, 5 min), N-glycans of high-mannose- and hybrid-type were detached from glycopeptides using 7 mU endo-β-*N*-acetylglucosaminidase H (Endo H) from *Escherichia coli* (Roche Applied Science) and digestion was carried out in 200 μL of 25 mM NaH_2PO_4/Na_2HPO_4 buffer at pH 5.6 and overnight at 37°C. Released N-glycans were isolated from the peptide moiety using C18 Extract-Clean™ cartridges (Alltech) and the N-glycan, as well as the remaining glycopeptide fraction was eluted and collected. The eluted N-glycans were desalted with carbograph Extract-Clean columns (Alltech) and evaporated to dryness. The eluted glycopeptides were also evaporated to dryness, dissolved in 300 μL of 20 mM NaH_2PO_4/Na_2HPO_4 (pH 7.0), and 1.5 U peptide-N4-(*N*-acetyl-β-glucosaminyl) asparagine amidase F (PNGase F; Roche Applied Science) from *Flavobacterium meningosepticum* were added to this glycopeptide solution for 8 h at 37°C to detach the complex-type N-glycans. Digestion was continued overnight by addition of a second aliquot of 1 U PNGase F. Released N-glycans were isolated from the peptide moiety using C18 Extract-Clean cartridges. The eluted N-glycans were desalted using carbograph Extract-Clean columns and evaporated to dryness.

Exoglycosidase digestions of N-glycans

The N-glycans of high-mannose- and hybrid-type were dissolved in 50 mM sodium acetate (pH 5.0; Merck) and digested for 18 h at 37°C using the following exoglycosidases consecutively with different concentrations: 3 U/mL *Arthrobacter ureafaciens* neuraminidase (Roche Applied Science), 0.2 U/mL β(1–4) galactosidase from *Streptococcus pneumoniae* (Prozyme), 4 U/mL β-*N*-acetylhexosaminidase recombinant from *S. pneumoniae* and expressed in *E. coli* (Prozyme), and 20 U/mL α-mannosidase from *Canavalia ensiformis* (Jack bean; Sigma-Aldrich). Complex-type N-glycans were also dissolved in 50 mM sodium acetate (pH 5.0) and digested for 18 h at 37°C using the following exoglycosidases consecutively with different concentrations: 3 U/mL *A. ureafaciens* neuraminidase, 1 U/mL bovine testes β-galactosidase, 6 U/mL β-*N*-acetylhexosaminidase recombinant from *S. pneumoniae* and expressed in *E. coli,* and to determine core-fucosylated structures, 2.3 U/mL bovine kidney α(1–2,3,4,6) fucosidase (all Prozyme). After inhibition at 95°C for 5 min, samples were permethylated and lyophilized.

Permethylation and MALDI-TOF-MS

Permethylation was performed in dimethyl sulfoxide (Merck) using sodium hydroxide and methyl iodide (Sigma-Aldrich) as described previously [30,31]. Chloroform (Merck) was then added and the chloroform phase was washed with water until the water phase became neutral. The chloroform phase was finally evaporated under reduced pressure and samples were dissolved in 75% aqueous acetonitrile (VWR) for MALDI-TOF measurements. N-glycans were analyzed on an Ultraflex III TOF/TOF mass spectrometer (Bruker Daltonics) equipped with a smartbeam-II™ laser and a LIFT-MS/MS facility. Measurements were carried out in the positive ionization mode. After a delayed extraction time of 10 ns, the ions were accelerated with 25 kV voltage. External calibration was performed using a dextran ladder. 0.5 μL of the sample was mixed directly on a ground steel target in a 1:1 ratio (v/v) with 10 mg/mL matrix superdihydroxybenzoic acid (Sigma-Aldrich) dissolved in 10% acetonitrile. Spectra were analyzed using the Glyco-Peakfinder software and assigned N-glycan structures were built with the GlycoWorkbench software [32,33].

Statistical analysis

Data were expressed as mean and standard error of mean. Student *t*-test was performed with SigmaStat software (Systat), to test expressed genes for their statistical significance ($^*P < 0.05$, $^{**}P < 0.01$, $^{***}P < 0.001$). Mann-Whitney *U* test was used to assess statistically significant changes of N-glycan structures during differentiation using SPSS 18.0 software (SPSS) ($^*P \leq 0.05$).

Results

Isolation, culture and verification of human MSCs

MSCs were isolated from bone marrow aspirates of three different donors and in P0 they showed a typical fibroblast-like morphology (Fig. 1A). During subsequent cultures up to P3, MSCs maintained this spindle-shaped morphology and cultures appeared homogeneous (Fig. 1B). In P3, MSCs were trypsinized and viability of detached cells was determined by trypan blue staining. The mean percentage of viable cells was 98.46% ± 0.23% ($n = 3$ donors: 98.69%, 98.46%, and 98.23%). Cells were analyzed by FACS to determine their MSC surface antigen pattern and as expected, they were CD44, CD73, CD90, CD105, CD166 positive, and CD14, CD34, CD45 negative (Fig. 1C). High cell viability and presentation of the glycoproteins CD44, CD90, CD105, and CD166 also indicated intact cell membranes with glycoproteins. MSCs verified using FACS were then used for examination of N-glycosylation and adipogenic differentiation.

Adipogenic potential of human MSCs

Human MSCs were directed into the adipogenic lineage to determine the glycosylation profile of adipogenically differentiated MSCs. As confirmed by oil red O staining, after 5 days, adipogenically stimulated MSCs started to form lipid droplets (Fig. 2A). In contrast, noninduced control cultures did not form any lipid droplets (Fig. 2B). In induced cultures, lipid formation reached a peak value after 15 days (Fig. 2C). Control cultures were still oil red O negative (Fig. 2D). On molecular level, the adipogenic marker genes *PPARG* (Fig. 2E) and *FABP4* (Fig. 2F) expression was significantly higher in induced cultures than in primary (day 0) or control (unstimulated) cultures. In conclusion, histology and qPCR confirmed adipogenic differentiation. Afterwards, for N-glycan analysis, the adipogenically differentiated MSCs were isolated from their fat matrix by trypsinization, and viability of detached cells was determined applying trypan blue

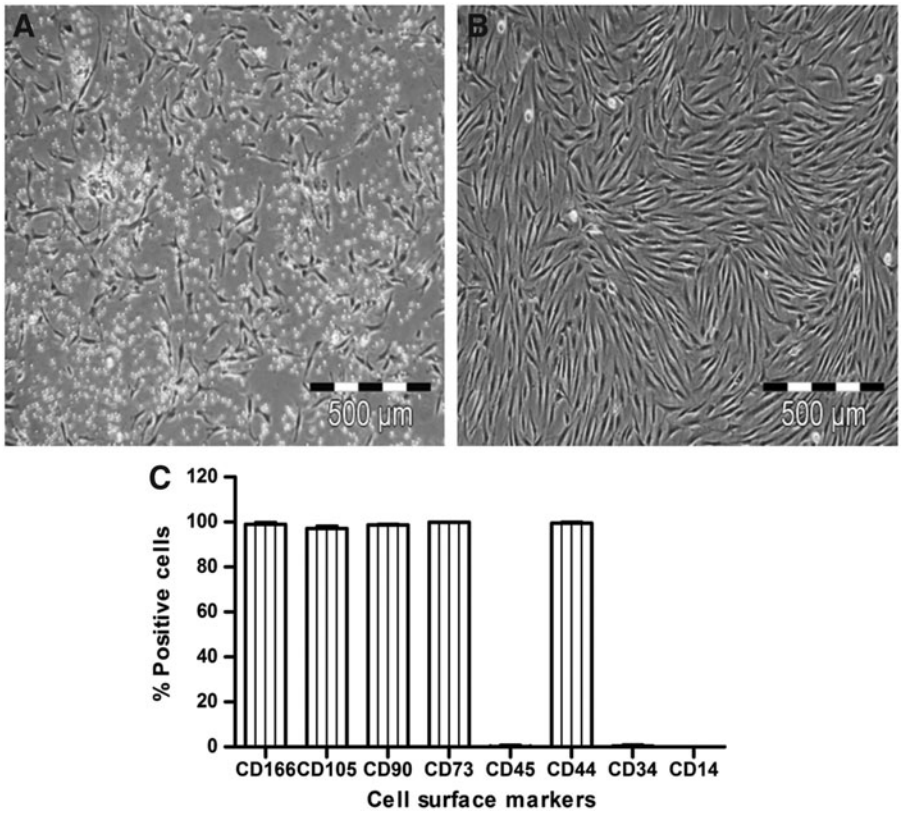

FIG. 1. Isolation, culture expansion, and verification of human bone marrow mesenchymal stem cells (MSCs). **(A)** In passage 0 (P0), freshly isolated human MSCs appeared as individual, fibroblast-like cells. **(B)** During culture expansion up to P3, they showed uniform growth characteristics and still maintained a fibroblast-like morphology. **(C)** In fluorescence-activated cell sorting analysis, P3 cells from three donors were positive for the typical MSC antigens CD44, CD73, CD90, CD105, and CD166 and negative for the hematopoietic cell markers CD14, CD34, and CD45.

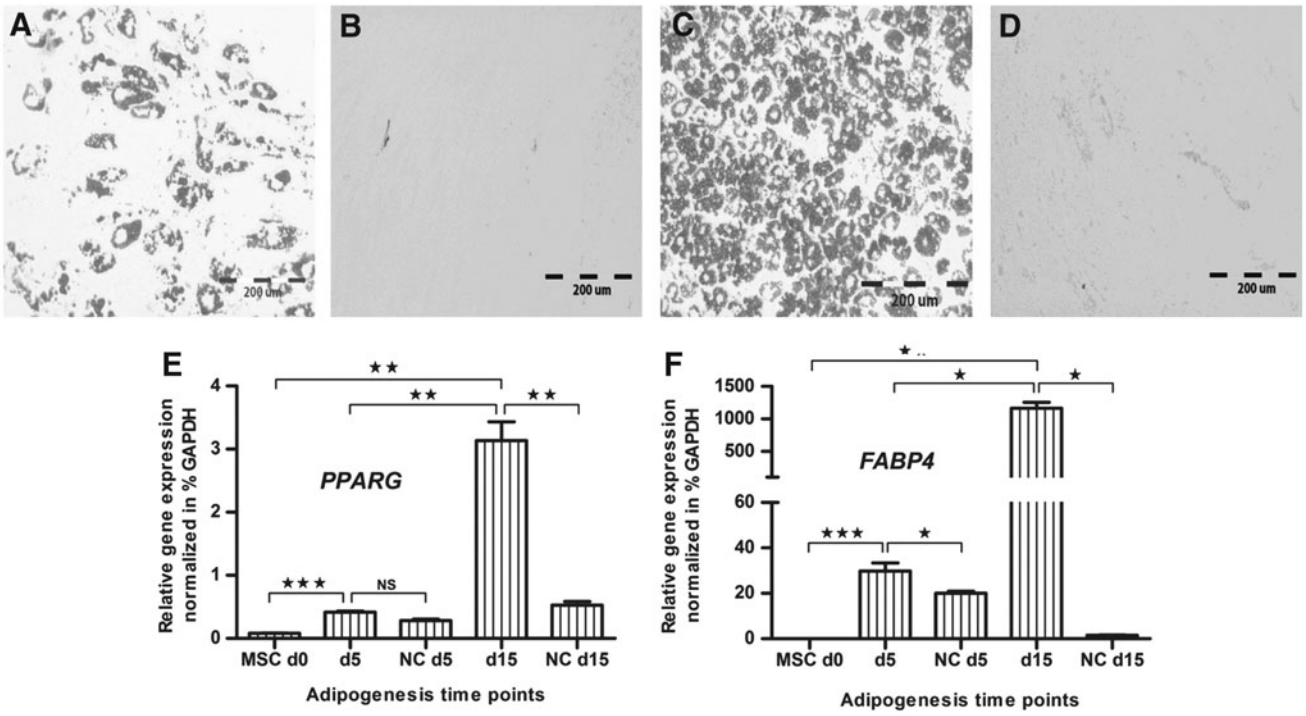

FIG. 2. Adipogenic differentiation of human MSCs. **(A)** MSCs were induced into the adipogenic lineage and at day 5, adipogenesis was assessed by oil red O staining of lipid droplets. **(B)** At day 5, unstimulated control MSCs (NC) did not form any lipid droplets. **(C)** At day 15, the number of oil red O stained lipid droplets was increased, **(D)** whereas the control cultures did not form any lipid droplets. **(E)** Real-time polymerase chain reaction revealed that the adipogenic marker genes peroxisome proliferator-activated receptor gamma (*PPARG*), and **(F)** fatty acid binding protein-4 (*FABP4)* were expressed significantly higher in induced cultures than in primary (day 0) or control (not stimulated) cultures ($^{*}P < 0.05$, $^{**}P < 0.01$, $^{***}P < 0.001$). Bar: 200 µm. NC, negative control.

staining. The mean percentage of viable cells from 5 days adipogenically differentiated cultures was 98.24% ± 0.12% ($n = 3$ donors: 98.12%, 98.36% and 98.24%) and from 15 days adipogenically differentiated cultures 96.99% ± 0.68% ($n = 3$ donors: 96.39%, 98.87% and 97.73%).

Analysis strategy for N-glycans

To analyze the N-glycome of undifferentiated and adipogenically differentiated human bone marrow-derived MSCs ($n = 3$ donors), their membrane glycoproteins were first isolated from cell pellets by membrane extraction. Then, the membrane glycoproteins were trypsinized to improve the efficiency of the subsequent endoglycosidase digestion. Subsequently, N-glycans were enzymatically released with Endo H, which cleaves high-mannose- and hybrid-type N-glycans. N-glycans were isolated from the sample by C18 solid phase extraction, yielding an N-glycan fraction (high-mannose- and hybrid-type N-glycans) and a glycopeptide fraction. Glycopeptides were further treated with PNGase F to release the remaining N-glycans; namely the complex-type N-glycans. This approach of Endo H digestion followed by PNGase F digestion was used here as it allows a good detection of complex-type N-glycans. High-mannoses usually represent the majority of the N-glycan pool and therefore, our method to separate high-mannose structures from complex-type structures ensures improved detection of complex-type N-glycans. Both Endo H and PNGase F digests were purified and analyzed separately. Permethylation was carried out before MALDI-TOF-MS to neutralize the negative charges of sialic acids to measure both acidic and neutral glycan structures in the positive ionization mode simultaneously [34,35].

The identified structures were verified by exoglycosidase digestions and by MALDI-TOF/TOF fragmentation. Digestions were done using different exoglycosidases in sequence: *A. ureafaciens* neuraminidase, β(1–4) galactosidase from *S. pneumoniae*, β-*N*-acetylhexosaminidase recombinant from *S. pneumoniae* and expressed in *E. coli*, α-mannosidase from *C. ensiformis* (Endo H-released N-glycans) and *A. ureafaciens* neuraminidase, bovine testes β-galactosidase, β-*N*-acetylhexosaminidase recombinant from *S. pneumoniae* expressed in *E. coli* and bovine kidney α(1–2,3,4,6) fucosidase (PNGase F-released N-glycans).

N-glycome of MSCs and its changes during adipogenic differentiation

Endo H cleaves asparagine-linked high-mannose- and hybrid-type N-glycans between the two N-acetyglucosamine (GlcNAc) subunits of the chitobiose core. Endo H-released N-glycans were purified using reversed-phase C18 and carbograph cartridges, permethylated, and measured by means of MALDI-TOF-MS. A representative spectrum is shown in Fig. 3A. Mean relative abundances, calculated from three different biological replicates, are presented in Fig. 3B and Table 1. The N-glycan profiles of the three different MSC donors were highly similar, as shown by the small deviations in the observed glycan profiles (Fig. 3B). Asterisks indicate statistical

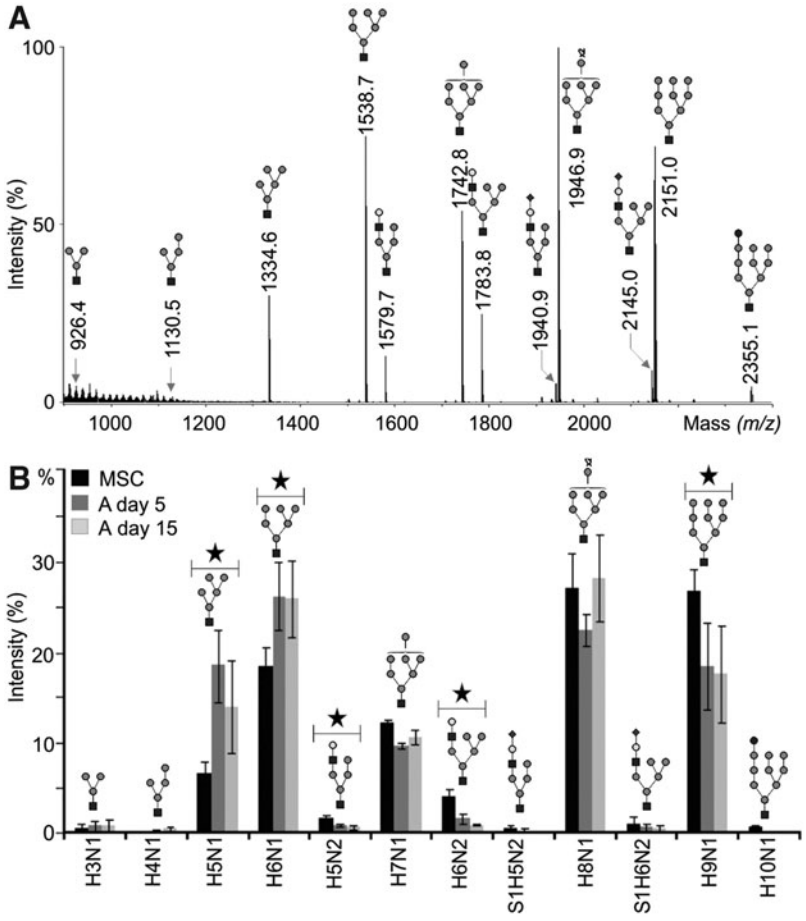

FIG. 3. Matrix-assisted laser desorption-ionization-time of flight mass spectrometry (MALDI-TOF-MS) of endo-β-*N*-acetylglucosaminidase H (Endo H)-released N-glycans. Glycoproteins were isolated from undifferentiated and adipogenically differentiated MSCs **(A)** using membrane extraction. N-glycans of high-mannose- and hybrid-type were then enzymatically cleaved with Endo H, permethylated, and measured by MALDI-TOF-MS. **(A)** A representative mass spectrum of Endo H-released N-glycans of undifferentiated human MSCs. **(B)** The average relative amounts of all Endo H-released N-glycans of undifferentiated human MSCs (*black*) and adipogenically differentiated MSCs **(A)** at day 5 (*dark gray*) and day 15 (*light gray*) derived from three different preparations. *Asterisks* mark statistical significant differences between the two sample groups undifferentiated MSCs and 15 days adipogenically differentiated MSCs according to the Mann-Withney *U* test ($^*P \leq 0.05$). The *black square* represents *N*-acetylglucosamine, *gray circle* mannose, *white circle* galactose, *black circle* glucose and *black diamond N*-acetylneuraminic acid. H, hexose; N, *N*-acetylhexosamine; S, *N*-acetylneuraminic acid.

Table 1. The Average Relative Amounts of Endo H-Released N-Glycans of Undifferentiated and Adipogenically Differentiated (A) Human Mesenchymal Stem Cells on Day 5 and 15 of Differentiation Derived from Three Different Donors

Endo H-released N-glycans				
m/z	*Composition*	*% in MSCs*	*% in A (day 5)*	*% in A (day 15)*
926.4	H3N1	0.61	0.76	0.81
1130.5	H4N1	0.20	0.34	0.49
1334.6	H5N1	6.63	18.53	13.93
1538.7	H6N1	18.48	26.20	25.89
1579.7	H5N2	1.65	0.87	0.61
1742.8	H7N1	12.14	9.61	10.62
1783.8	H6N2	4.14	1.63	0.98
1940.9	H5N2S1	0.51	0.33	0.20
1946.9	H8N1	27.17	22.43	28.20
2145.0	H6N2S1	1.12	0.67	0.56
2151.0	H9N1	26.70	18.44	17.56
2355.1	H10N1	0.63	0.20	0.14

Endo-H, endo-β-*N*-acetylglucosaminidase H; MSCs, mesenchymal stem cells; H, hexose; N, *N*-acetylhexosamine; S, *N*-acetylneuraminic acid.

significant differences between the two sample groups undifferentiated MSCs and 15 days adipogenically differentiated MSCs according to Mann-Withney *U* test ($P \leq 0.05$).

The mass spectrometric data revealed 12 high-mannose- and hybrid-type N-glycan structures; seven of them are high-mannose-type N-glycans with the composition H3-9N1 (*m/z* 926.4, 1130.5, 1334.6, 1538.7, 1742.8, 1946.9 and 2151.0, respectively). The relative amount of overall high-mannose-type N-glycans was 5.7% higher in 15 days adipogenically differentiated MSCs when compared to undifferentiated MSCs. Smaller high-mannose-type N-glycans namely, H5N1 (*m/z* 1334.6) and H6N1 (*m/z* 1538.7) were particularly overexpressed in 5 days and 15 days adipogenically differentiated MSCs, with a relative amount of 14% for H5N1 and 26% for H6N1 in 15 days adipogenically differentiated MSCs ($P < 0.05$). In contrast, a significant decrease of more than 9% was observed for the high-mannose-type structure H9N1 (*m/z* 2151.0) and it ocurred after 15 days of differentiation. Four hybrid-type N-glycans, namely H5N2 (*m/z* 1579.7), H6N2 (*m/z* 1783.8), S1H5N2 (*m/z* 1940.9) and S1H6N2 (*m/z* 2145.0), constituted 2.4% of the total N-glycome of 15 days adipogenically differentiated MSCs. The relative amount of these structures decreased during differentiation since they were 5% underexpressed in 15 days adipogenically differentiated MSCs when compared to the N-glycome of undifferentiated MSCs. The changes in relative amount of neutral hybrid-type N-glycans H5N2 (*m/z* 1579.7) and H6N2 (*m/z* 1783.8) in 15 days adipogenically differentiated MSCs and undifferentiated MSCs were statistically significant. In addition, a glycan of the composition H10N1 was detected in trace amounts at *m/z* 2355.1, which was verified as the monoglucosylated precursor H10N1 high-mannose-type N-glycan that has been previously reported to be present in human blood serum [36]. In general, the average relative amounts of Endo H-released N-glycans of undifferentiated and adipogenically differentiated MSCs (5 or 15 days) were more different than those of 5 and 15 days adipogenically differentiated MSCs (Fig. 3B; Table 1). In contrast, the mass spectra of all the three groups were qualitatively almost similar. As shown in the next paragraph, this was also true for PNGase F-digested glycopeptides.

Endo H-digested glycopeptides were subjected to PNGase F-digestion to release complex-type N-glycans. A representative mass spectrum of the resulting N-glycosylation profile of human MSCs is shown in Fig. 4. About 100 different N-glycan signals were detected with MALDI-TOF-MS (Table 2). The relative abundance of the 48 most abundant N-glycans is presented in Fig. 5A and B. A small amount of hybrid- and high-mannose-type N-glycans, 3% and 2%, respectively, was detected in the pool of PNGase F-released N-glycans, indicating that Endo H-digestion of the corresponding glycopeptides was about 95% complete. Some of them were carrying just one core GlcNAc, showing that a low portion of the Endo H-derived N-glycans remained bound to the C18 column and thus, eluted in the glycopeptide fraction that was then treated with PNGase F.

The data from mass spectrometry profiling revealed that fucosylated bi-, tri- and tetraantennary complex-type N-glycans dominated the N-glycan profiles of undifferentiated MSCs and 5 and 15 days adipogenically differentiated MSCs.

Fucosylation. Fucosylated structures were predominantly monofucosylated at the reducing GlcNAc residue. A characteristic feature of 5 and 15 days adipogenically differentiated MSCs was the increased abundance of biantennary N-glycans, such as the nonfucosylated N-glycans S1H5N4 (*m/z* 2431.2) and S2H5N4 (*m/z* 2792.3), as well as the fucosylated N-glycans H3N4F1 (*m/z* 1835.9), H5N4F3 (*m/z* 2592.3), S1H5N4F1 (*m/z* 2605.3) and S2H5N4F1 (*m/z* 2966.4). For instance, the biantennary fucosylated N-glycans H3N4F1, H5N4F3 and S2H5N4F1 were significantly overexpressed in 15 days adipogenically differentiated MSCs.

Antennarity. Triantennary N-glycans were less abundant in 5 and 15 days adipogenically differentiated MSCs. Fucosylated triantennary structures like H6N5F1 (*m/z* 2693.3) and S1H6N5F1 (*m/z* 3054.5) were also less abundant in the N-glycome of 5 and 15 days adipogenically differentiated MSCs when compared to undifferentiated MSCs. The N-glycans H6N5F1 (*m/z* 2693.3) and S1H6N5 (*m/z* 2880.4) were significantly underexpressed in 15 days adipogenically differentiated MSCs. Moreover, the amount of tetraantennary N-glycans was also decreased in the N-glycome of 5 and 15 days adipogenically differentiated. Remarkably, fucosylated tetraantennary structures were at least 10% less abundant in 15 days adipogenically differentiated MSCs than in undifferentiated MSCs. For instance, the fully galactosylated N-glycans H7N6F1 (*m/z* 3142.5), S1H7N6F1 (*m/z* 3503.7) and S2H7N6F1 (*m/z* 3864.9) were clearly more enriched in undifferentiated MSCs. The N-glycans H7N6F1 (*m/z* 3142.5), S1H7N6 (*m/z* 3329.6) and S1H7N6F1 (*m/z* 3503.7) were significantly underexpressed in 15 days adipogenically differentiated MSCs. Poly-LacNAc N-glycans, such as H6N5 (*m/z* 2519.2), H6N5F1 (*m/z* 2693.3), H7N6F1 (*m/z* 3142.5), and S1H7N6F1 (*m/z* 3503.7) were predominantly found in N-glycans of human MSCs and were very little in adipogenically differentiated MSCs.

Sialylation. More than half of the PNGase F-released N-glycans of MSCs were found to be sialylated. They were

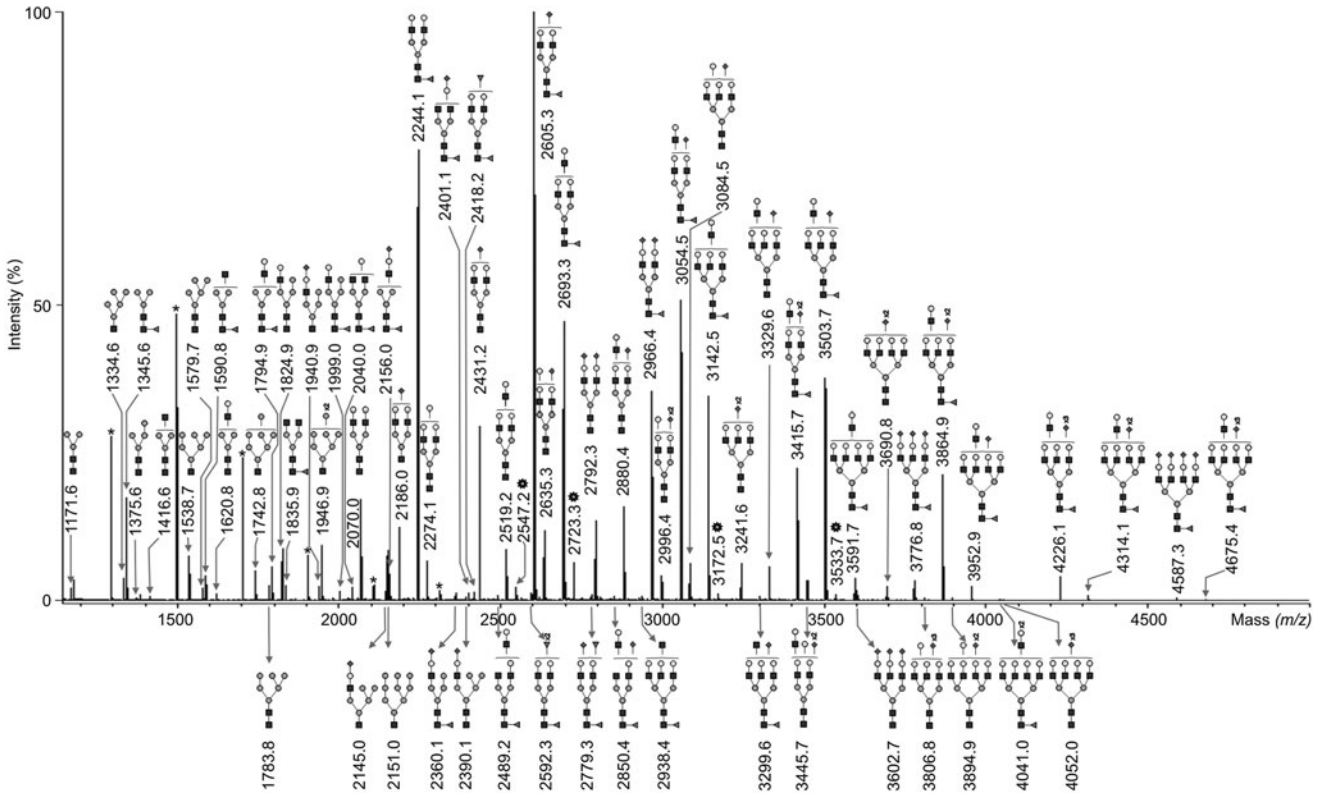

FIG. 4. MALDI-TOF-MS of peptide-N4-(*N*-acetyl-β-glucosaminyl) asparagine amidase F (PNGase F)-released complex-type N-glycans. Glycoproteins were isolated from undifferentiated and adipogenically differentiated MSCs. After isolation of high-mannose- and hybrid-type N-glycans by Endo H digestion, digested glycopeptides were subjected to PNGase F digestion to release complex-type N-glycans, permethylated and measured by MALDI-TOF-MS. A representative mass spectrum of PNGase F-released N-glycans of undifferentiated human MSCs is shown together with the 70 most abundant structures. Polyhexose contaminations are marked with *asterisks* and are negligible. Unidentified peaks were marked with *complex asterisks*. The *black square* represents *N*-acetylglucosamine, *gray circle* mannose, *white circle* galactose, *black triangle* fucose and *black diamond N*-acetylneuraminic acid.

predominantly monosialylated although di-, tri- and tetrasialylated N-glycans were also present. Thus, most of the sialylated N-glycans were found to be just partially sialylated and minority of them were fully sialylated. Moreover, the presence of fully sialylated structures decreased with increasing antennarity. The amount of sialylated N-glycans in 15 days adipogenically differentiated MSCs was 16.5% higher than in undifferentiated MSCs. This was mainly affected by an increased amount of sialylated biantennary structures, such as S1H5N4F1 (*m/z* 2605.3) and S2H5N4F1 (*m/z* 2966.4) in 5 and 15 days adipogenically differentiated MSCs.

Verification of the identified N-glycan structures in undifferentiated and adipogenically differentiated MSCs. Verification of the most abundant N-glycan structures was done using specific exoglycosidases (Supplementary Tables S1 and S2; Supplementary Data are available online at www.liebertpub.com/scd) in combination with MALDI-TOF/TOF-MS fragmentation that was performed in the positive-ion mode. A representative MALDI-TOF/TOF mass spectrum is presented in Fig. 6 for the N-glycan signal F1H5N4S1 (*m/z* 2605.3). Sialylated Endo H-released N-glycans were digested using neuraminidase (Supplementary Table S1). As a result, the two peaks of the composition S1H5N2 (*m/z* 1940.9) and S2H6N2 (*m/z* 2145.0) shifted to H5N2 (*m/z* 1579.7) and H6N2 (*m/z* 1783.8), respectively. Further shift was observed after β(1–4)-galactosidase digestion followed by β-*N*-acetylhexosaminidase digestion. These results confirmed the presence of hybrid-type structures at *m/z* 1579.7 and *m/z* 1783.8, and of a sialylated antenna in S1H5N2 (*m/z* 1940.9) and S2H6N2 (*m/z* 2145.0). In addition, a diagnostic fragment ion S1H1N1 at *m/z* 847.2 confirmed the sialylated antenna in S1H5N2 (*m/z* 1940.9) and S2H6N2 (*m/z* 2145.0). Fragmentation analysis of H5N2 (*m/z* 1579.7) and H6N2 (*m/z* 1783.8) revealed a signal at *m/z* 486.0 (H1N1) that indicated the presence of hybrid-type structures. The rest of the signals that remained after β-*N*-acetylhexosaminidase digestion were sensitive to α-mannosidase treatment as their signals disappeared from the MALDI-TOF mass spectrum. In addition, a signal at *m/z* 1334.6 corresponding to H5N1 remained after α-mannosidase digestion. Therefore, H10N1 (*m/z* 2355.1) was assigned to the monoglucosylated N-glycan precursor Glc1Man9GlcNAc1 of the N-glycan H10N1 (*m/z* 2355.1). After fragmentation of H10N1, the monoglucosylated antennae was confirmed by the presence of the diagnostic fragment ions H4 at *m/z* 852.5 and H3 at *m/z* 649 that indicates the presence of an antenna bearing four hexoses.

Sialylated N-glycans obtained from PNGase F digestion were digested with neuraminidase (Supplementary Table S2). Digestion with β-galactosidase and β-*N*-acetylhexosaminidase proved the presence of galactose and GlcNAc in

Table 2. The Average Relative Amounts of All PNGase F-Released N-Glycans of Undifferentiated and Adipogenically Differentiated (A) Human Mesenchymal Stem Cells on Day 5 and Day 15 of Differentiation Derived from Three Different Donors

PNGase F-released N-glycans									
m/z	*Composition*	*% in MSCs*	*% in A (day 5)*	*% in A (day 15)*	*m/z*	*Composition*	*% in MSCs*	*% in A (day 5)*	*% in A (day 15)*
1171.6	H3N2	0.21	0.30	0.26	2751.3	S2H6N3	0.04	0.02	0.00
1334.6	H5N1	0.16	0.20	0.11	2779.3	S1H5N4F2	0.10	0.13	0.27
1345.6	H3N2F1	0.68	0.70	0.83	2792.3	S2H5N4	0.79	0.86	1.21
1375.6	H4N2	0.05	0.06	0.04	2809.3	S1H6N4F1	0.05	0.04	0.04
1416.7	H3N3	0.07	0.14	0.21	2839.4	S1H7N4	0.02	0.01	0.00
1538.7	H6N1	0.38	0.34	0.34	2850.4	S1H5N5F1	0.08	0.04	0.09
1579.7	H5N2	0.12	0.11	0.07	2867.4	H6N5F2	0.04	0.07	0.07
1590.8	H3N3F1	0.25	0.54	0.90	2880.4	S1H6N5	1.69	0.79	0.48
1620.8	H4N3	0.08	0.12	0.12	2938.4	H6N6F1	0.06	0.04	0.06
1661.8	H3N4	0.01	0.02	0.04	2953.4	S1H5N4F3	0.04	0.12	0.24
1742.8	H7N1	0.23	0.13	0.16	2966.4	S2H5N4F1	4.11	7.27	9.09
1783.8	H6N2	0.10	0.03	0.03	2996.4	S2H6N4	0.28	0.73	0.51
1794.9	H4N3F1	0.40	0.29	0.19	3054.5	S1H6N5F1	8.77	5.86	5.24
1824.9	H5N3	0.83	2.00	0.62	3084.5	S1H7N5	0.47	0.33	0.23
1835.9	H3N4F1	0.24	0.71	1.87	3112.5	N6H6F2	0.01	0.01	0.00
1865.9	H4N4	0.04	0.06	0.11	3142.5	H7N6F1	5.58	0.64	0.43
1940.9	S1H5N2	0.13	0.23	0.14	3200.5	S2H7N4	0.01	0.01	0.00
1946.9	H8N1	0.65	0.40	0.59	3215.6	H6N5F4	0.01	0.00	0.00
1968.9	H4N3F2	0.01	0.02	0.02	3228.6	S1H6N5F2	0.02	0.04	0.07
1981.9	S1H4N3	0.03	0.05	0.07	3241.6	S2H6N5	0.44	0.28	0.41
1999.0	H5N3F1	0.16	0.05	0.05	3257.6	S1H7N5F1	0.00	0.00	0.06
2029.0	H6N3	0.05	0.05	0.03	3299.6	S1H6N6F1	0.08	0.02	0.02
2040.0	H4N4F1	0.23	0.22	0.26	3316.6	H7N6F2	0.02	0.00	0.00
2070.0	H5N4	2.12	3.62	2.52	3329.6	S1H7N6	0.58	0.15	0.07
2081.0	H3N5F1	0.02	0.07	0.19	3357.6	H6N7F2	0.03	0.12	0.18
2145.0	S1H6N2	0.08	0.07	0.08	3415.7	S2H6N5F1	2.10	3.87	4.04
2151.0	H9N1	0.45	0.25	0.30	3445.7	S2H7N5	0.27	0.30	0.20
2156.0	S1H4N3F1	0.22	0.27	0.30	3503.7	S1H7N6F1	5.29	1.03	0.96
2186.0	S1H5N3	0.89	2.92	1.47	3591.7	H8N7F1	0.37	0.04	0.11
2214.1	H4N4F2	0.05	0.04	0.06	3602.7	S3H6N5	0.14	0.34	2.08
2227.1	S1H4N4	0.02	0.03	0.06	3660.8	S2H6N6F1	0.02	0.00	0.00
2244.1	H5N4F1	16.81	18.42	12.41	3690.8	S2H7N6	0.19	0.03	0.05
2274.1	H6N4	0.56	0.62	0.31	3776.8	S3H6N5F1	0.36	0.27	1.91
2285.1	H4N5F1	0.01	0.02	0.01	3806.8	S3H7N5	0.06	0.09	0.16
2360.1	S1H5N3F1	0.09	0.03	0.07	3864.9	S2H7N6F1	2.19	0.59	1.22
2390.1	S1H6N3	0.04	0.08	0.05	3894.9	S2H8N6	0.05	0.02	0.04
2401.1	S1H4N4F1	0.09	0.12	0.17	3952.9	S1H8N7F1	0.14	0.02	0.17
2418.2	H5N4F2	0.16	0.34	0.53	3964.9	S4H6N5	0.00	0.02	0.22
2431.2	S1H5N4	2.91	4.33	5.41	4041.0	H9N8F1	0.07	0.00	0.00
2448.2	H6N4F1	0.03	0.04	0.04	4052.0	S3H7N6	0.03	0.00	0.00
2461.2	G1H5N4	0.03	0.05	0.10	4140.0	S2H8N7	0.01	0.00	0.00
2478.2	H7N4	0.01	0.01	0.00	4226.1	S3H7N6F1	0.82	0.17	0.98
2489.2	H5N5F1	0.09	0.14	0.15	4314.1	S2H8N7F1	0.15	0.01	0.10
2519.2	H6N5	2.40	0.74	0.30	4402.2	S1H9N8F1	0.05	0.00	0.03
2592.3	H5N4F3	0.24	0.71	1.45	4587.3	S4H7N6F1	0.15	0.03	0.41
2605.3	S1H5N4F1	20.36	30.85	32.31	4675.4	S3H8N7F1	0.04	0.00	0.08
2635.3	S1H6N4	0.86	1.62	1.10	4764.4	S2H9N8F1	0.00	0.00	0.08
2693.3	H6N5F1	10.52	3.43	2.10					

PNGase F, peptide-N4-(*N*-acetyl-β-glucosaminyl) asparagine amidase F; H, hexose; N, *N*-acetylhexosamine; F, deoxyhexose; S, *N*-acetylneuraminic acid.

the corresponding N-glycans. After digestion with β-*N*-acetylhexosaminidase, the two structures H3N2 (*m/z* 1171.6) and H3N2F1 (*m/z* 1345.6) remained, showing that every fucosylated N-glycan of the pool bears one α(1–6)-linked fucose at the asparagine-linked GlcNAc residue. In addition, the detection of the diagnostic fragment ions N1F1 at *m/z* 474.0 and N2F1 at *m/z* 719.2 proved core-fucosylation for instance in S1H5N4F1 (*m/z* 2605.3) (Fig. 6). The most abundant biantennary N-glycans H5N4F1 (*m/z* 2244.1) and S1H5N4F1 (*m/z* 2605.3) were found to be core-fucosylated in undifferentiated MSCs and adipogenically differentiated MSCs since their fragmentation generated the two diagnostic

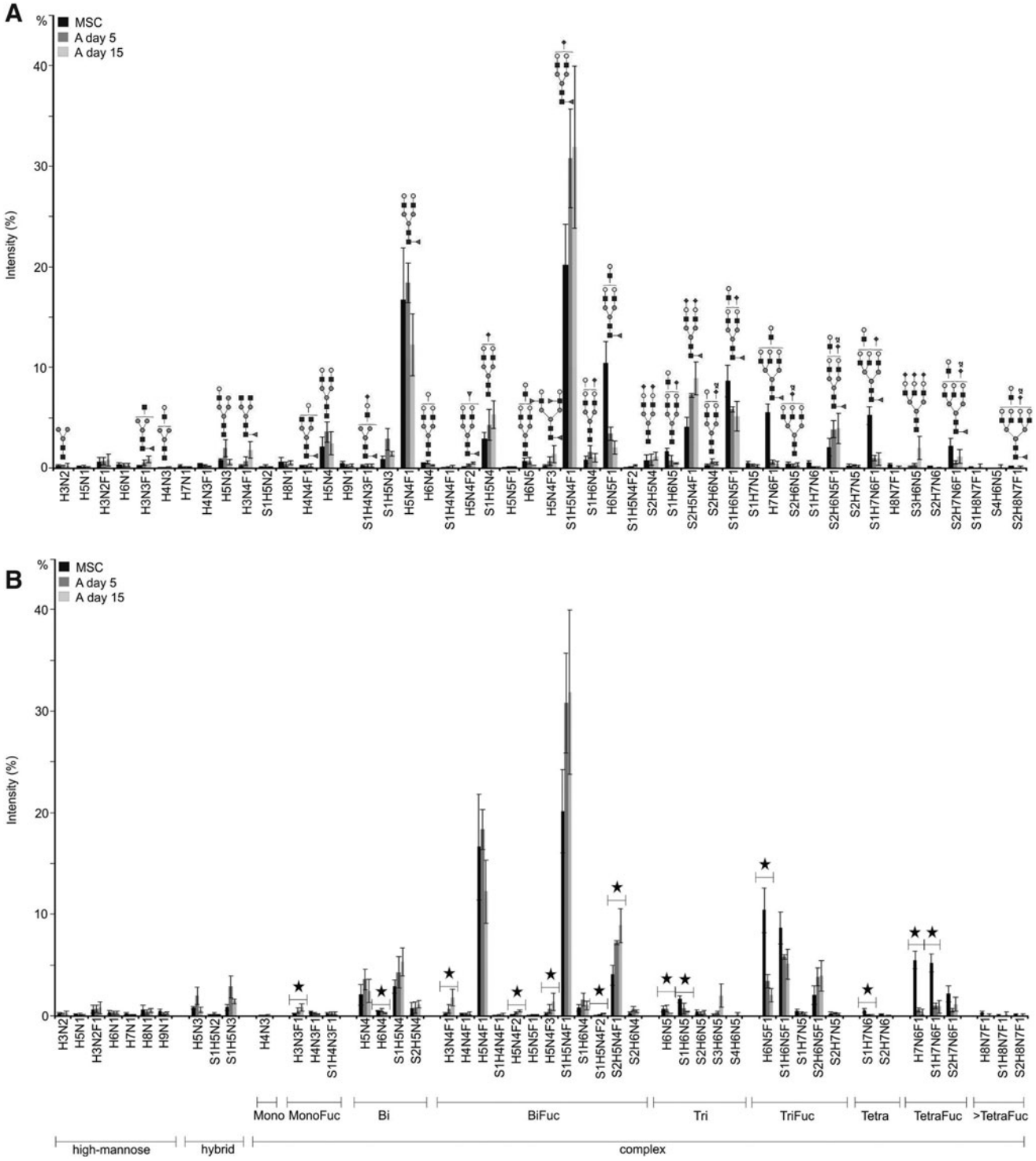

FIG. 5. Quantification of PNGase F-released N-glycans with MALDI-TOF-MS. **(A)** The average relative amounts of the 48 most abundant PNGase F-released N-glycans of undifferentiated human MSCs (*black*) and adipogenically differentiated MSCs **(A)** at day 5 (*dark gray*) and day 15 (*light gray*) derived from three different preparations, **(B)** grouped according to their N-glycan type, antennarity and fucosylation. Statistical significant difference between the two sample groups undifferentiated MSCs and 15 days adipogenically differentiated MSCs was assessed using Mann-Whitney *U* test ($^*P \leq 0.05$). The *black square* represents *N*-acetylglucosamine, *dark gray circle* mannose, *white circle* galactose, *black triangle* fucose and *black diamond* *N*-acetylneuraminic acid. H, hexose; N, *N*-acetylhexosamine; F, deoxyhexose; S, *N*-acetylneuraminic acid.

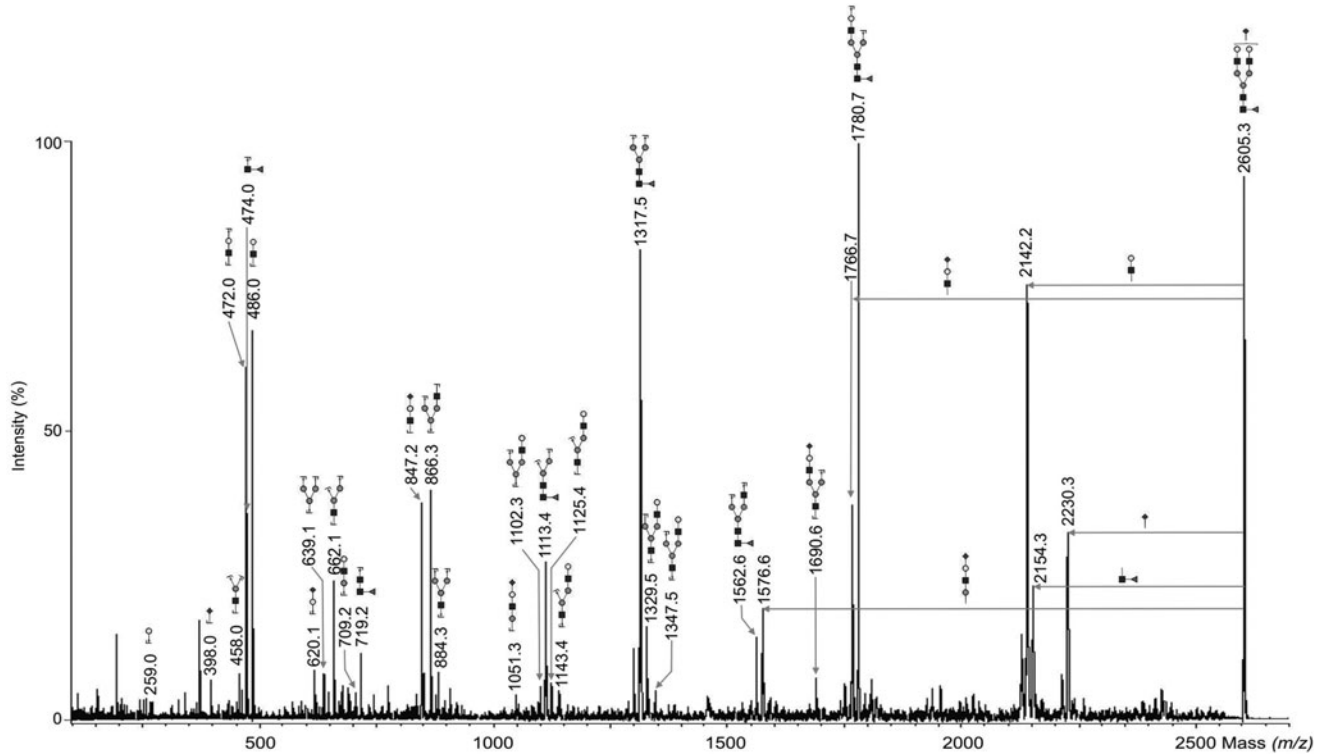

FIG. 6. An example of a MALDI-TOF/TOF mass spectrum of *m/z* 2605.3 of the composition S1H5N4F1 derived from human MSCs. *Black square* represents *N*-acetylglucosamine, *dark gray circle* mannose, *white circle* galactose, *black triangle* fucose and *black diamond N*-acetylneuraminic acid.

ions N1F1 at *m/z* 474.0 and N2F1 at *m/z* 719.2. A representative MALDI-TOF/TOF mass spectrum is presented in Fig. 6 for the N-glycan signal *m/z* 2605.3, which represents a biantennary, monosialylated, and core-fucosylated structure with the composition F1H5N4S1. The diagnostic fragment ions S1H1N1 at *m/z* 847.2 and S1H2N1 at *m/z* 620.1 confirmed the presence of a sialylated antenna in S1H5N4F1 (*m/z* 2605.3) (Fig. 6), S2H5N4F1 (*m/z* 2966.4), S1H6N5F1 (*m/z* 3054.5), S2H6N5F1 (*m/z* 3415.7), S1H7N6F1 (*m/z* 3503.7), S3H6N5F1 (*m/z* 3776.8), S2H7N6F1 (*m/z* 3864.9), and S3H7N6F1 (*m/z* 4226.1).

One signal G1H5N4 at *m/z* 2461.2 was found to correspond to an N-glycan, which bears *N*-glycolylneuraminic acid and was also observed in a previous study [37] in MSCs, but this glycan was only found as a trace. This contaminant is most likely stemming from cell culture media that contain animal-derived components [38,39]. After neuraminidase digestion, the N-glycan structures H6N4 (*m/z* 2274.1) and H7N5 (*m/z* 2723.3), which correspond to a trigalactosylated biantennary N-glycan and a tetragalactosylated triantennary N-glycan, remained. The digestion of these N-glycans with bovine testes β-galactosidase confirmed the presence of only β-linked galactoses. Therefore, it was concluded that the signals at *m/z* 2274.1, *m/z* 2635.3, *m/z* 2996.4, *m/z* 3084.5, *m/z* 3445.7, *m/z* 3806.8, and *m/z* 3894.9 corresponded to structures of the form $S_xH_{y+2}N_y$ (Supplementary Table S2).

We found a LacNAc motif in the tri- or tetraantennary structures H5N5F1 (*m/z* 2489.2), H6N5 (*m/z* 2519.2), H6N5F1 (*m/z* 2693.3), S1H5N5F1 (*m/z* 2850.4), S1H6N5 (*m/z* 2880.4), S1H6N5F1 (*m/z* 3054.5), H7N6F1 (*m/z* 3142.5), S1H7N6 (*m/z* 3329.6), S2H6N5F1 (*m/z* 3415.7), S1G1H6N5F1 (*m/z* 3445.7), S1H7N6F1 (*m/z* 3503.7), H8N7F1 (*m/z* 3591.7), S2H7N6F1 (*m/z* 3864.9), S1H8N7F1 (*m/z* 3952.9), S3H7N6F1 (*m/z* 4226.1) and S2H8N7F1 (*m/z* 4314.1). The presence of poly-LacNAc in these structures was verified by the diagnostic fragment ion H2N2 at *m/z* 935.2. The poly-LacNAc signals were predominantly found in N-glycans of undifferentiated human MSCs and were minimal in adipogenically differentiated MSCs. N-glycans like H8N7F1 (*m/z* 3591.7), S1H8N7F1 (*m/z* 3952.9) and S2H8N7F1 (*m/z* 4314.1) were additionally found to be core-fucosylated and the presence of a sialylated antenna in S1H8N7F1 (*m/z* 3952.9) and S2H8N7F1 (*m/z* 4314.1) was proven by the diagnostic fragment ions S1H1N1 at *m/z* 847.2 and S1H1 at *m/z* 620.1.

Discussion

Targeting glycan-based stage specific markers for MSCs and their adipogenically differentiated progeny, we investigated in this study the N-glycosylation profile of human bone marrow-derived MSCs during adipogenic development on the qualitative and quantitative levels. To our knowledge, this is the first report on the N-glycome of early (day 5) and late (day 15) adipogenically differentiated MSCs.

For adipogenesis, we performed a standardized and reproducible assay, in which MSCs were stimulated for up to 15 days with an adipogenic cocktail consisting of insulin, dexamethasone, indomethacin and 3-isobutyl-1-methylxanthine [3,12]. Then, cell membrane glycoproteins were isolated and N-glycans were released and analyzed by MALDI-TOF-MS combined with exoglycosidase digestions. We focused on N-glycans because among all types of glycosylations, they

are the most common type of post-translational protein modifications.

High-mannose-type N-glycans were the predominant type of N-glycans in human MSCs and their adipogenically differentiated progeny. They were more abundant in adipogenically differentiated MSCs, where small high-mannose-type N-glycans with three to six mannoses were found to be overexpressed. Previous studies revealed that besides human MSCs and their osteogenically counterparts [37], human embryonic [40] and hematopoietic stem and progenitor cells [41] also contain high amounts of high-mannose-type N-glycans on their cell surface. We found that short high-mannose-type N-glycans H5N1 and H6N1 were significantly more abundant in adipogenically differentiated MSCs, whereas the larger high-mannose-type N-glycan H9N1 was significantly decreased in relative amount in 15 days adipogenically differentiated MSCs. Heiskanen et al. reported as well that high-mannose-type N-glycans dominate the N-glycan profile of undifferentiated MSCs when compared to their osteogenically differentiated counterparts, in which mainly N-glycans with more than six mannoses were enriched [37]. They also showed that smaller high-mannose-type N-glycans were relatively more abundant in osteogenically differentiated MSCs. In summary, our data and the data from Heiskanen et al. [37] reveal that high-mannose-type N-glycans bearing at least six mannoses were more abundant in undifferentiated MSCs and may therefore, be characteristic for undifferentiated human MSCs when compared to osteogenically or adipogenically differentiated MSCs.

Interestingly, we detected the monoglucosylated H10N1 high-mannose-type N-glycan, which is a characteristic feature of improperly folded nascent glycoproteins in the endoplasmic reticulum. Glycoproteins with monoglucosylated glycan moiety remain in the endoplasmic reticulum until proper folding is achieved within the calnexin/calreticulin cycle [42]. Others showed that the monoglucosylated H10N1 high-mannose-type N-glycan was found to be in human embryonic stem cells as well [43]. The presence of the monoglucosylated H10N1 may therefore, be a typical feature of stem cells.

Hybrid-type N-glycans were found to be the less abundant type of N-glycosylation in undifferentiated human MSCs and adipogenically differentiated MSCs. We observed neutral, sialylated, as well as fucosylated hybrid-type structures. Our mass spectrometric data revealed that neutral hybrid-type N-glycans H5N2 and H6N2 were significantly overexpressed in undifferentiated human MSCs. In contrast, a previous study by Heiskanen et al. revealed that neutral hybrid-type N-glycans were enriched in osteogenically differentiated MSCs [37]. These differences are probably due to the fact that we performed endoglycosidase digestions after tryptic digestion of the (glyco)proteins, which improves the accessibility of endoglycosidases to the reducing end of glycans. On the contrary, Heiskanen et al. [37] did not specify how the PNGase F digestion was performed.

Regarding the complex-type N-glycans, we found a decrease in fucosylation and branching in adipogenically differentiated MSCs. A significant increase of biantennary fucosylated N-glycans H3N4F1, H5N4F3, and S2H5N4F1 was observed in 15 days adipogenically differentiated MSCs, whereas undifferentiated human MSCs contained significantly more triantennary H6N5F1 and S1H6N5 and tetra-antennary H7N6F1, S1H7N6, and S1H7N6F1 N-glycans than adipogenically differentiated MSCs. Our results are corroborated by Morad et al. [44], who showed using lectin staining of membrane extracts that adipogenically differentiation of MSCs was accompanied by a decreased level of antennarity of complex-type N-glycans, namely of tri- and tetra-antennary structures. In addition, they proved that the level of these structures was increased in osteogenically differentiated MSCs when compared to undifferentiated MSCs. However, in the latter mentioned study, glycoanalysis of membrane proteins was performed using lectin microarrays, showing that different methods lead to similar results [44]. In contrast, Heiskanen et al. reported that the acidic N-glycan profile of MSCs contained relatively more of the larger complex-type N-glycans (five GlcNAc or more) and more N-glycans with two or more fucose residues when compared to their osteogenically counterparts [37]. In our study, fucosylated N-glycans were found to bear at least one fucose at the core. However, the most abundant fucosylated N-glycans were found to contain just one fucose that is α(1–6)-linked to the asparagine-linked GlcNAc residue of the N-glycan.

According to our MALDI-TOF-MS data, the overall sialylation was increased in adipogenically differentiated MSCs. Heiskanen et al. found that complex-type N-glycans lacking *N*-acetylneuraminic acids were enriched in osteogenically differentiated MSCs [37]. Combined together, the results indicate that the variation of sialylation may be dependent on whether the MSCs were adipogenically or osteogenically differentiated.

Linear poly-LacNAcs were mainly found in undifferentiated MSCs, indicating that this epitope is characteristic for undifferentiated MSCs, as has been previously reported [37]. High-molecular weight poly-LacNAcs are present in human embryonal carcinoma cells, where they are assumed to play roles in the interactions on the same membrane. Moreover, large branched poly-LacNAc, which are expressed in mouse embryonic stem cells and early embryonic cells are supposed to participate in cell survival by increasing the interaction of membrane molecules within the membrane [24]. Furthermore, it has been shown that poly-LacNAcs can change their structure from linear chains in fetal blood cells into branched chains in the adult [45]. Poly-LacNAc epitopes are thought to interact with lectins in a multivalent fashion, such as with β-galactoside binding lectins, known as galectins. Galectins are involved in many cell adhesions and signaling phenomena and studies revealed that they have a higher affinity for poly-LacNAcs than for single LacNAc units, suggesting that the function of LacNAc epitopes is influenced by their structure [37,46–48].

In conclusion, several studies revealed that the glycosylation of different stem cells, such as pluripotent embryonic [40,43,49,50] or multipotent adult stem cells [37,41], has characteristic features. Most of these studies rely on staining of carbohydrates with lectins and antibodies in combination with techniques like FACS, western blotting, microarray, and immunohistochemistry [20,51]. However, the specificity of lectins and antibodies is limited, which might lead to the loss of important structural information. MALDI-TOF-MS is a promising tool to study the N-glycome of stem cells and to search for differentiation associated glycan structures [39,41]. We have investigated and verified the N-glycome of bone marrow MSCs and their adipogenically differentiated progeny with this technique in combination with exoglycosidase

digestions. The results show that the N-glycome of adipogenically differentiated human MSCs was clearly less fucosylated and branched than the one of undifferentiated human MSCs. We propose N-glycans like H6N5F1 and H7N6F1 as candidate MSC markers for undifferentiated MSCs and N-glycans like H3N4F1 and H5N4F3 as potential markers for adipogenically differentiated MSCs. We also found N-glycans that are potential candidate markers to discriminate between 5 and 15 days adipogenically differentiated MSCs. In the context of soft tissue engineering, markers are important to verify culture homogeneity of MSCs and their adipogenically differentiated progeny, to monitor the progress of MSC development during adipogenesis and to analyze quality parameter like cell distribution in new formed adipose tissue. As concluded, mass spectrometry is a useful tool to gain the exact structural information on glycosylation but it requires lot of material to be used in the frame of routine quality control. Therefore, as already mentioned, our strategy is to generate specific antibodies that detect development stage specific N-glycans. Moreover, in future studies, our mass spectrometry results could be translated into a lectin assay, which allows an easier detection of N-glycans. Potential candidates are *Phaseolus vulgaris* Leukoagglutinin and *Datura stramonium* Agglutinin as they recognize specifically galactosylated tri- and tetra-antennary N-glycans. To conclude, our results show that modulation of cell surface glycosylation is a promising stem cells biomarker.

Acknowledgments

The authors thank Elena Frisch, Josè Bernadino Gonzalez, Thomas Häupl, Berthold Hoppe, Barbara Walewska, and Stefanie Wedepohl for their support and useful comments. This study was supported by grants from the Investitionsbank Berlin and the European Regional Development Fund (grants no: 10147244 and 10147246).

Author Disclosure Statement

M.S. works as a consultant for BioTissue Technologies GmbH (Freiburg, Germany). The company develops autologous tissue transplants for the regeneration of bone and cartilage. He is also a shareholder of CellServe GmbH (Berlin, Germany) and BioRetis GmbH (Berlin, Germany). The product interests of both companies have no connection with the topics discussed here. All authors declare no financial or personal relationship with persons or organizations that would inappropriately influence this scientifically oriented in vitro study. We therefore declare no competing financial interests.

References

1. Ringe J, GR Burmester and M Sittinger. (2012). Regenerative medicine in rheumatic disease-progress in tissue engineering. Nat Rev Rheumatol 8:493–498.
2. Brunt KR, RD Weisel and RK Li. (2012). Stem cells and regenerative medicine - future perspectives. Can J Physiol Pharmacol 90:327–335.
3. Pittenger MF, AM Mackay, SC Beck, RK Jaiswal, R Douglas, JD Mosca, MA Moorman, DW Simonetti, S Craig and DR Marshak. (1999). Multilineage potential of adult human mesenchymal stem cells. Science 284:143–147.
4. Ji JF, BP He, ST Dheen and SS Tay. (2004). Interactions of chemokines and chemokine receptors mediate the migration of mesenchymal stem cells to the impaired site in the brain after hypoglossal nerve injury. Stem Cells 22: 415–427.
5. Yu J, M Li, Z Qu, D Yan, D Li and Q Ruan. (2010). SDF-1/CXCR4-mediated migration of transplanted bone marrow stromal cells toward areas of heart myocardial infarction through activation of PI3K/Akt. J Cardiovasc Pharmacol 55:496–505.
6. Caplan AI and D Correa. (2011). The MSC: an injury drugstore. Cell Stem Cell 9:11–15.
7. Giordano A, U Galderisi and IR Marino. (2007). From the laboratory bench to the patient's bedside: an update on clinical trials with mesenchymal stem cells. J Cell Physiol 211:27–35.
8. Huang L and A Burd. (2012). An update review of stem cell applications in burns and wound care. Indian J Plast Surg 45:229–236.
9. Mohal JS, HD Tailor and WS Khan. (2012). Sources of adult mesenchymal stem cells and their applicability for musculoskeletal applications. Curr Stem Cell Res Ther 7:103–109.
10. Gronthos S, SE Graves, S Ohta and PJ Simmons. (1994). The STRO-1+ fraction of adult human bone marrow contains the osteogenic precursors. Blood 84:4164–4173.
11. Kolf CM, E Cho and RS Tuan. (2007). Mesenchymal stromal cells. Biology of adult mesenchymal stem cells: regulation of niche, self-renewal and differentiation. Arthritis Res Ther 9:204.
12. Menssen A, T Haupl, M Sittinger, B Delorme, P Charbord and J Ringe. (2011). Differential gene expression profiling of human bone marrow-derived mesenchymal stem cells during adipogenic development. BMC Genomics 12:461.
13. Lanctot PM, FH Gage and AP Varki. (2007). The glycans of stem cells. Curr Opin Chem Biol 11:373–380.
14. Haltiwanger RS and JB Lowe. (2004). Role of glycosylation in development. Annu Rev Biochem 73:491–537.
15. Varki A. (1993). Biological roles of oligosaccharides: all of the theories are correct. Glycobiology 3:97–130.
16. Perillo NL, ME Marcus and LG Baum. (1998). Galectins: versatile modulators of cell adhesion, cell proliferation, and cell death. J Mol Med (Berl) 76:402–412.
17. Rudd PM, MR Wormald, RL Stanfield, M Huang, N Mattsson, JA Speir, JA DiGennaro, JS Fetrow, RA Dwek and IA Wilson. (1999). Roles for glycosylation of cell surface receptors involved in cellular immune recognition. J Mol Biol 293:351–366.
18. Helenius A and M Aebi. (2004). Roles of N-linked glycans in the endoplasmic reticulum. Annu Rev Biochem 73:1019–1049.
19. Varki A. (2006). Nothing in glycobiology makes sense, except in the light of evolution. Cell 126:841–845.
20. Tateno H, N Uchiyama, A Kuno, A Togayachi, T Sato, H Narimatsu and J Hirabayashi. (2007). A novel strategy for mammalian cell surface glycome profiling using lectin microarray. Glycobiology 17:1138–1146.
21. Spiro RG. (2002). Protein glycosylation: nature, distribution, enzymatic formation, and disease implications of glycopeptide bonds. Glycobiology 12:43R–56R.
22. Yu RK and M Yanagisawa. (2006). Glycobiology of neural stem cells. CNS Neurol Disord Drug Targets 5:415–423.
23. Yanagisawa M and RK Yu. (2007). The expression and functions of glycoconjugates in neural stem cells. Glycobiology 17:57R–74R.

24. Muramatsu T and H Muramatsu. (2004). Carbohydrate antigens expressed on stem cells and early embryonic cells. Glycoconj J 21:41–45.
25. Close BE, SS Mendiratta, KM Geiger, LJ Broom, LL Ho and KJ Colley. (2003). The minimal structural domains required for neural cell adhesion molecule polysialylation by PST/ST8Sia IV and STX/ST8Sia II. J Biol Chem 278:30796–30805.
26. Kim DS, DR Lee, HS Kim, JE Yoo, SJ Jung, BY Lim, J Jang, HC Kang, S You, et al. (2012). Highly pure and expandable PSA-NCAM-positive neural precursors from human ESC and iPSC-derived neural rosettes. PLoS One 7:e39715.
27. Chomczynski P. (1993). A reagent for the single-step simultaneous isolation of RNA, DNA and proteins from cell and tissue samples. Biotechniques 15:532–534, 536–537.
28. Pfaffl MW. (2001). A new mathematical model for relative quantification in real-time RT-PCR. Nucleic Acids Res 29:e45.
29. Lieke T, D Grobe, V Blanchard, D Grunow, R Tauber, M Zimmermann-Kordmann, T Jacobs and W Reutter. (2011). Invasion of *Trypanosoma cruzi* into host cells is impaired by N-propionylmannosamine and other N-acylmannosamines. Glycoconj J 28:31–37.
30. Wada Y, P Azadi, CE Costello, A Dell, RA Dwek, H Geyer, R Geyer, K Kakehi, NG Karlsson, et al. (2007). Comparison of the methods for profiling glycoprotein glycans—HUPO Human Disease Glycomics/Proteome Initiative multi-institutional study. Glycobiology 17:411–422.
31. Dell A, AJ Reason, KH Khoo, M Panico, RA McDowell and HR Morris. (1994). Mass spectrometry of carbohydrate-containing biopolymers. Methods Enzymol 230:108–132.
32. Maass K, R Ranzinger, H Geyer, CW von der Lieth and R Geyer. (2007). "Glyco-peakfinder"—de novo composition analysis of glycoconjugates. Proteomics 7:4435–4444.
33. Ceroni A, K Maass, H Geyer, R Geyer, A Dell and SM Haslam. (2008). GlycoWorkbench: a tool for the computer-assisted annotation of mass spectra of glycans. J Proteome Res 7:1650–1659.
34. Wedepohl S, M Kaup, SB Riese, M Berger, J Dernedde, R Tauber and V Blanchard. (2010). N-glycan analysis of recombinant L-Selectin reveals sulfated GalNAc and GalNAc-GalNAc motifs. J Proteome Res 9:3403–3411.
35. Reinke SO, M Bayer, M Berger, S Hinderlich and V Blanchard. (2012). The analysis of N-glycans of cell membrane proteins from human hematopoietic cell lines reveals distinctions in their pattern. Biol Chem 393:731–747.
36. Frisch E, M Kaup, K Egerer, A Weimann, R Tauber, M Berger and V Blanchard. (2011). Profiling of endo H-released serum N-glycans using CE-LIF and MALDI-TOF-MS—application to rheumatoid arthritis. Electrophoresis 32:3510–3515.
37. Heiskanen A, T Hirvonen, H Salo, U Impola, A Olonen, A Laitinen, S Tiitinen, S Natunen, O Aitio, et al. (2009). Glycomics of bone marrow-derived mesenchymal stem cells can be used to evaluate their cellular differentiation stage. Glycoconj J 26:367–384.
38. Martin MJ, A Muotri, F Gage and A Varki. (2005). Human embryonic stem cells express an immunogenic nonhuman sialic acid. Nat Med 11:228–232.
39. Heiskanen A, T Satomaa, S Tiitinen, A Laitinen, S Mannelin, U Impola, M Mikkola, C Olsson, H Miller-Podraza, et al. (2007). N-glycolylneuraminic acid xenoantigen contamination of human embryonic and mesenchymal stem cells is substantially reversible. Stem Cells 25:197–202.
40. Wearne KA, HC Winter, K O'Shea and IJ Goldstein. (2006). Use of lectins for probing differentiated human embryonic stem cells for carbohydrates. Glycobiology 16:981–990.
41. Hemmoranta H, T Satomaa, M Blomqvist, A Heiskanen, O Aitio, J Saarinen, J Natunen, J Partanen, J Laine and T Jaatinen. (2007). N-glycan structures and associated gene expression reflect the characteristic N-glycosylation pattern of human hematopoietic stem and progenitor cells. Exp Hematol 35:1279–1292.
42. Parodi AJ. (2000). Protein glucosylation and its role in protein folding. Annu Rev Biochem 69:69–93.
43. An HJ, P Gip, J Kim, S Wu, KW Park, CT McVaugh, DV Schaffer, CR Bertozzi and CB Lebrilla. (2012). Extensive determination of glycan heterogeneity reveals an unusual abundance of high mannose glycans in enriched plasma membranes of human embryonic stem cells. Mol Cell Proteomics 11:M111 010660.
44. Morad V, M Pevsner-Fischer, S Barnees, A Samokovlisky, L Rousso-Noori, R Rosenfeld and D Zipori. (2008). The myelopoietic supportive capacity of mesenchymal stromal cells is uncoupled from multipotency and is influenced by lineage determination and interference with glycosylation. Stem Cells 26:2275–2286.
45. Fukuda M, MN Fukuda and S Hakomori. (1979). Developmental change and genetic defect in the carbohydrate structure of band 3 glycoprotein of human erythrocyte membrane. J Biol Chem 254:3700–3703.
46. Leffler H, S Carlsson, M Hedlund, Y Qian and F Poirier. (2004). Introduction to galectins. Glycoconj J 19:433–440.
47. Stowell SR, CM Arthur, P Mehta, KA Slanina, O Blixt, H Leffler, DF Smith and RD Cummings. (2008). Galectin-1, -2, and -3 exhibit differential recognition of sialylated glycans and blood group antigens. J Biol Chem 283:10109–10123.
48. Stowell SR, M Dias-Baruffi, L Penttila, O Renkonen, AK Nyame and RD Cummings. (2004). Human galectin-1 recognition of poly-N-acetyllactosamine and chimeric polysaccharides. Glycobiology 14:157–167.
49. Satomaa T, A Heiskanen, M Mikkola, C Olsson, M Blomqvist, M Tiittanen, T Jaatinen, O Aitio, A Olonen, et al. (2009). The N-glycome of human embryonic stem cells. BMC Cell Biol 10:42.
50. Venable A, M Mitalipova, I Lyons, K Jones, S Shin, M Pierce and S Stice. (2005). Lectin binding profiles of SSEA-4 enriched, pluripotent human embryonic stem cell surfaces. BMC Dev Biol 5:15.
51. Tao SC, Y Li, J Zhou, J Qian, RL Schnaar, Y Zhang, IJ Goldstein, H Zhu and JP Schneck. (2008). Lectin microarrays identify cell-specific and functionally significant cell surface glycan markers. Glycobiology 18:761–769.

Address correspondence to:
Dr. Véronique Blanchard
Institute of Laboratory Medicine, Clinical Chemistry and Pathobiochemistry
Charité-Universitätsmedizin Berlin
Augustenburger Platz 1
Berlin 13353
Germany

E-mail: veronique.blanchard@charite.de

Received for publication February 21, 2013
Accepted after revision July 4, 2013
Prepublished on Liebert Instant Online July 7, 2013